



HAL
open science

Preparation of nitro-phenothiazine-based oxime esters as dual photo/thermal initiators for 3D printing

Xiaoxiang Zhang, Xiaotong Peng, Di Zhu, Yijun Zhang, Marie Le Dot, Serife Ozen, Michael Schmitt, Fabrice Morlet-Savary, Pu Xiao, Frédéric Dumur, et al.

► To cite this version:

Xiaoxiang Zhang, Xiaotong Peng, Di Zhu, Yijun Zhang, Marie Le Dot, et al.. Preparation of nitro-phenothiazine-based oxime esters as dual photo/thermal initiators for 3D printing. *Journal of Polymer Science*, In press, 10.1002/pol.20230327 . hal-04513933

HAL Id: hal-04513933

<https://hal.science/hal-04513933v1>

Submitted on 20 Mar 2024

HAL is a multi-disciplinary open access archive for the deposit and dissemination of scientific research documents, whether they are published or not. The documents may come from teaching and research institutions in France or abroad, or from public or private research centers.


L'archive ouverte pluridisciplinaire **HAL**, est destinée au dépôt et à la diffusion de documents scientifiques de niveau recherche, publiés ou non, émanant des établissements d'enseignement et de recherche français ou étrangers, des laboratoires publics ou privés.



Distributed under a Creative Commons Attribution 4.0 International License

RESEARCH ARTICLE

Preparation of nitro-phenothiazine-based oxime esters as dual photo/thermal initiators for 3D printing

Xiaoxiang Zhang^{1,2,3} | Xiaotong Peng⁴ | Di Zhu⁴ | Yijun Zhang^{2,3} |
Marie Le Dot^{2,3} | Serife Ozen^{2,3} | Michael Schmitt^{2,3} |
Fabrice Morlet-Savary^{2,3} | Pu Xiao⁴ | Frédéric Dumur⁵ | Jacques Lalevée^{2,3} 

¹School of Textiles, Zhongyuan University of Technology, Zhengzhou, China

²Université de Haute-Alsace, CNRS, IS2M UMR 7361, Mulhouse, France

³Université de Strasbourg, France

⁴Research School of Chemistry, Australian National University, Canberra, ACT, Australia

⁵Aix Marseille Univ, CNRS, ICR, UMR 7273, Marseille, France

Correspondence

Pu Xiao, Research School of Chemistry, Australian National University, Canberra, ACT 2601, Australia.

Email: pu.xiao@anu.edu.au

Frédéric Dumur, Aix Marseille Univ, CNRS, ICR, UMR 7273, F-13397 Marseille, France.

Email: frederic.dumur@univ-amu.fr

Jacques Lalevée, Université de Haute-Alsace, CNRS, IS2M UMR 7361, F-68100 Mulhouse, France.

Email: jacques.lalevee@uha.fr

Funding information

CSC - China Scholarship Council, Grant/Award Number: 201902425004

Abstract

Nowadays, photopolymerization has spanned across all academic and industrial applications due to its appealing features such as energy saving, environmentally-friendly polymerization conditions, high monomer conversions, rapid polymerization kinetics and so on. Photoinitiator (PI), as a crucial component of the photoinitiating system (PIS) are capable of interacting with light efficiently, enabling to generate initiating species in mono or multicomponent systems. In this work, 13 phenothiazine-based oxime esters (OXEs) (never reported before) were synthesized and their photoinitiation abilities for the free radical photopolymerization (FRP) of acrylates were examined upon irradiation with LED@405 nm. Parallel to their photochemical reactivities, their abilities to initiate thermal polymerization processes were also investigated. Finally, these OXEs exhibited excellent photo/thermal initiation performances, demonstrating their dual initiation properties. Phenothiazine-based oxime esters can be used as PIs in 3D printing as well as thermal initiator in the manufacturing of carbon fiber composites.

KEYWORDS

free radical polymerization, oxime esters, phenothiazine, photoinitiators, photopolymerization, visible light

1 | INTRODUCTION

Photopolymerization has drawn more and more attention in the academic fields because it is a low-cost, convenient, low-toxic, environmental-friendly, and energy-saving technology.^{1,2} With regard to its numerous advantages, photopolymerization has been widely used in research fields,

including dentistry, 3D and 4D printing, coatings, and microelectronic fabrications.^{3–5} Photoinitiator (PI) is one of the most important key components in photopolymerization as it directly interacts with light, promoting the generation of initiating species. At present and considering the fast development of 3D printing, the design of PIs that can be used under near-UV or visible light irradiation becomes

This is an open access article under the terms of the [Creative Commons Attribution](https://creativecommons.org/licenses/by/4.0/) License, which permits use, distribution and reproduction in any medium, provided the original work is properly cited.

© 2023 The Authors. *Journal of Polymer Science* published by Wiley Periodicals LLC.

more and more important.^{5,6} Indeed, LEDs emitting at 405 nm are presently used in 3D printers. With the aim at increasing 3D printing speed, a number of highly reactive photoinitiating systems have been designed.^{5–8} However, many of them were multi-component systems consisting of an organic chromophore (often a dye), an onium salt and/or an amine.^{9,10} These combinations can induce photopolymerization process via intermolecular electron transfer. Nevertheless, the efficiency of these multicomponent systems is greatly affected by the interaction efficacy existing between the photosensitizer and the different additives,^{9,10} hence influencing monomer conversions. This issue can be addressed if monocomponent photoinitiating systems are used.¹¹

One compound fragmenting system is referred as type I photoinitiator.^{11,12} However, most of the Type I PIs only work efficiently under UV light,^{13,14} and only a few PIs, such as diphenyl (2,4,6-trimethylbenzoyl) phosphine oxide (TPO), phenylbis (2,4,6-trimethylbenzoyl)-phosphine oxide (BAPO) and 2-benzyl-2-(dimethylamino)-1-[4-(4-morpholinyl) phenyl]-1-butanone can be photoexcited with visible light.¹⁴ Therefore, the investigation of new photoinitiators that can be activated under near-UV or visible light is of great interest.¹⁵ Due to their high photo-reactivities, OXEs have gained increasing interests.^{11,15–17} Their photoinitiation process consists of two steps: (i) homolytic cleavage of the N—O bond and (ii) decarboxylation reaction of the aryloxy/alkyloxy radicals. To be a good type I PI, the N—O bond of OXEs must have an efficient cleavage process, and then the active free radicals are generated by decarboxylation.¹⁸ *O*-benzoyl- α -oxoamide (OXE01) and *O*-acetyloxime (OXE02) are two examples of commercial OXE Type I PIs. These structures can be photoexcited by the light around 330 nm, implying that these two structures exhibit low performances when exposed to near-UV light (e.g., LED@385 or 395 nm) or visible light (e.g., LED@405 nm).¹⁹ Therefore, there is an urgent need to develop effective OXE-based photoinitiators activable under mild photopolymerization conditions upon near-UV/visible light irradiation. Different photoinitiators based on other chromophores or wavelengths are also under development.^{20,21}

In our previous works, a number of OXEs with absorption maxima around 360 nm were proposed as photoinitiators and could be activated in the UV–visible range.^{22,23} A recent review gathering some progress on OXEs as LED photoinitiators can be found in Reference²² and references therein. Photoinitiation and thermal initiation abilities of these OXEs in trimethylolpropane triacrylate (TMPTA) were evaluated, and some of them furnished excellent monomer conversions and could achieve outstanding performance in direct laser write (DLW) experiments. These results motivated us to investigate and expand the family of OXEs that can cater to the demands of

various applications of photopolymerization.^{22–24} In this work, a series of nitrophenothiazine-based OXEs exhibiting a dual photo/thermal initiator behavior were presented and discussed.

As shown in Scheme 1, 13 nitrophenothiazine-based OXEs (from OXE-A to OXE-M) and the same chromophore without the oxime-ester moiety (OXE-N) were developed and synthesized in this study. Since the absorption of phenothiazine derivatives is located in the visible range, phenothiazine was employed as the chromophore in this investigation.²⁵ In order to improve the absorption in the visible range, a nitro group was connected to the phenothiazine core. For comparisons, OXE01 and OXE02 were used as benchmark photoinitiators. The chemical structures of the multifunctional monomer TMPTA and the benchmark PIs (OXE01 and OXE02) are shown in Scheme 2. Additionally, photoinitiation abilities and photophysical properties of the different OXEs were investigated using real-time Fourier transformed infrared (RT-FTIR), UV–visible absorption and electron spin resonance spin trapping (ESR-ST). Afterwards, direct laser write experiments were carried out to evaluate their future applications. Markedly, several OXEs demonstrated thermal initiation abilities through differential scanning calorimetry (DSC) analysis, and their corresponding fiber-filled composites were also successfully prepared via thermal polymerization coupled with photoinitiation for good curing of the top surface.

2 | EXPERIMENTAL PART

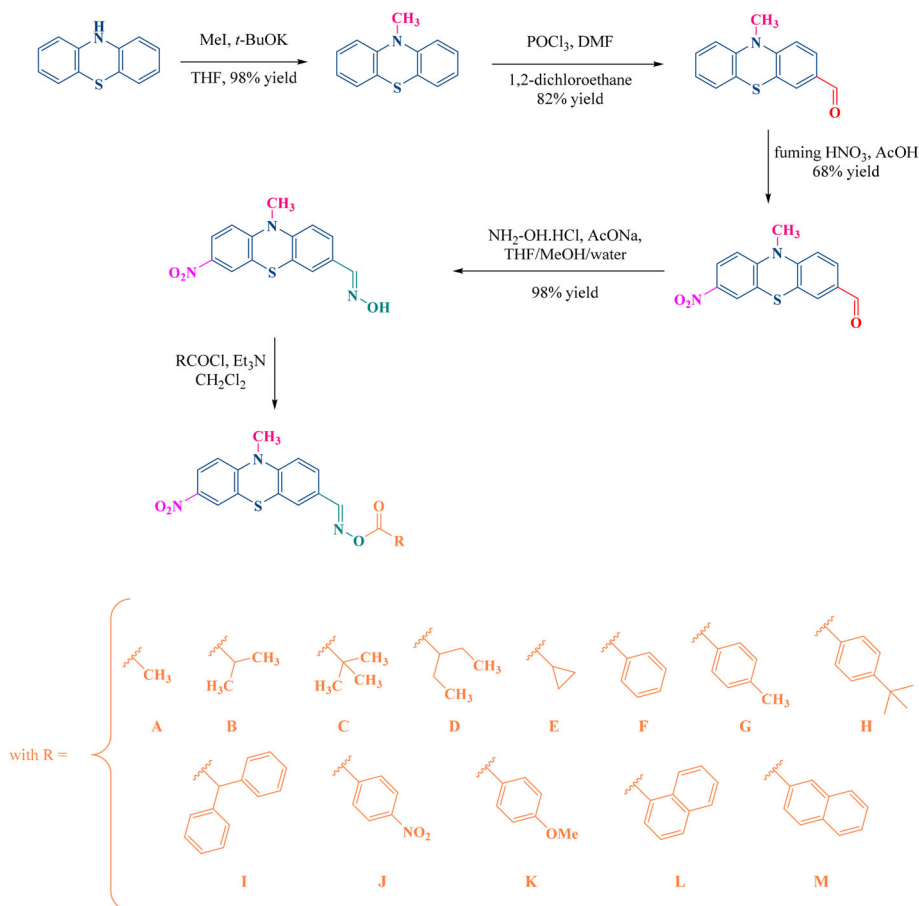
The experimental setups to characterize the photopolymerization processes are described in detail in [Supporting Information](#): (i) Real-Time Fourier Transformed Infrared Spectroscopy to follow the photopolymerization kinetics, (ii) the Differential scanning calorimetry (DSC) for thermal polymerization, and (iii) the Direct Laser Write (DLW) experiments for the spatial control of the reaction. The syntheses and the NMR characterizations of the new proposed photoinitiators are also given in [Supporting Information](#).

3 | RESULTS AND DISCUSSION

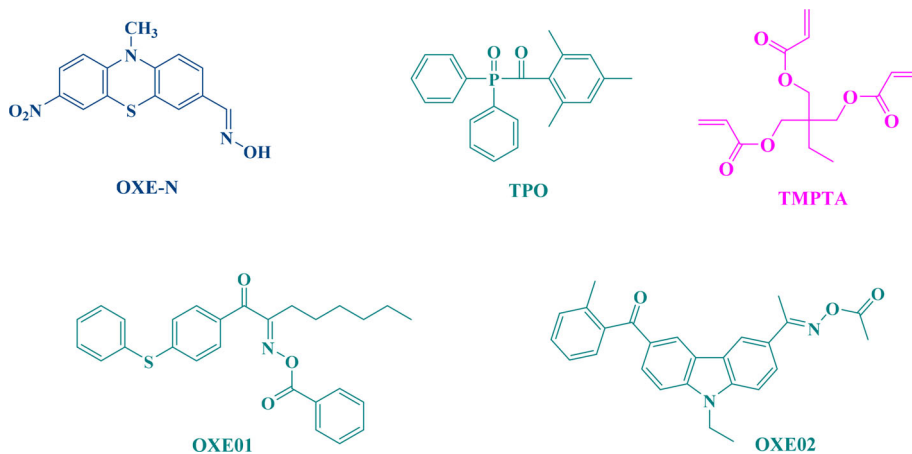
3.1 | Synthesis of phenothiazine-based oxime esters

Thirteen nitro-phenothiazine-based oxime esters never reported before were prepared in this work in five steps starting from phenothiazine. First, by alkylation of phenothiazine with iodomethane in the presence of a base, 10-methyl-10*H*-phenothiazine was obtained in 98% yield.

SCHEME 1 Synthetic routes of oxime esters (noted OXE-A to OXE-M), the oxime OXE-N (R = OH) is the compound before esterification.



SCHEME 2 Chemical structures of OXE-N (the benchmark chromophore without ester cleavable group), OXE01, OXE02, TPO, and TMPTA.



Then, by Vilsmeier Haak reaction in 1,2-dichloroethane as the solvent, 10-methyl-10H-phenothiazine-3-carbaldehyde was prepared in 82% yield. Nitration of phenothiazine using fuming nitric acid as the nitration agent in acetic acid furnished the targeted 10-methyl-7-nitro-10H-phenothiazine-3-carbaldehyde in 68% yield. 10-Methyl-7-nitro-10H-phenothiazine-3-carbaldehyde oxime was prepared in quantitative yield using hydroxylamine hydrochloride and sodium acetate using a mixture of solvents. Finally, oxime esters A-M were obtained by esterification of oxime with the appropriate acid chlorides using triethylamine as the base (see

Scheme 1). The different oxime esters were obtained with reaction yields ranging from 70% for H to 89% for G (see Supporting Information, S1.1–S1.17 and Table S1).

3.2 | Light absorption properties of the examined OXEs

The molar extinction coefficients obtained from UV transmittance experiments in acetonitrile solutions (concentration 1×10^{-4} mol/L) of the oxime/esters are

shown in Figure 1, the maximum molar extinction coefficients of OXEs are summarized in Table 1. The maximum molar extinction coefficient (ϵ_{\max}) of OXE-N is 2.2×10^4 L/(mol·cm), and its maximum absorption wavelength (λ_{\max}) is 376 nm. Compared to the oxime OXE-N, the oxime esters OXEs have a slight hypsochromic shift in absorbance, as well as lower ϵ_{\max} values. OXE-M had the smallest ϵ_{\max} , which is about 1.1×10^4 L/(mol·cm) at 372 nm. This clearly indicates an interaction of the R group with the absorbance of the PI which will clearly influence the initiation behavior. In addition, large steric groups seem to influence the absorption by affecting the intermolecular interaction of the chromophoric part and/or the side group in a complex way (e.g., for OXE-G and OXE-H). The absorption spectra of these OXEs overlapped with the emission spectrum of the near-UV (405 nm). Hence, these OXEs have the potential to be visible light (LED@405 nm) sensitive photoinitiators.

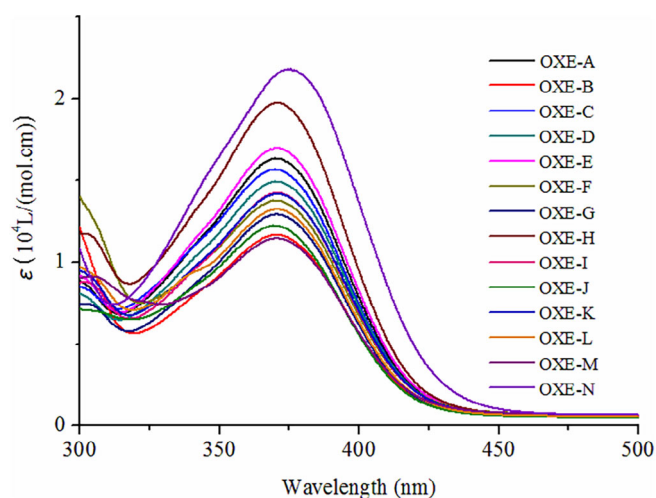


FIGURE 1 UV-Visible absorption spectra of the different OXEs in acetonitrile (1×10^{-4} mol/L).

3.3 | Photoinitiation abilities of OXEs

Polymerization profiles obtained with the different OXEs are given in Figure 2, and the “final” double bond conversion (FC) are gathered in Table 1. Interestingly, OXE-N without a cleavable group only showed weak photoinitiation ability and final conversion of 26% was obtained. Other OXEs showed variable photoinitiation abilities during the polymerization of TMPTA. Remarkably, OXE-A and OXE-D have the highest final function conversion (FC = 65%), which is very close to the reference TPO (FC = 69%, the same molecular amount of TPO as a reference/benchmark structure). OXE-J possessing a strong electron-withdrawing group (i.e., a nitrophenyl group) showed only a low final monomer conversion (FC = 40%). It was proposed that cleavage can occur more easily in OXEs with electrophilic groups than in other OXEs.²⁶ All OXEs containing an oxime ester group bearing an aromatic ring did not achieve high FCs as evidenced by OXE-F (48%), OXE-G (50%), OXE-H (54%), OXE-I (46%), OXE-K (49%), OXE-L (53%), and OXE-M (48%). The steric hindrance effect and the decarboxylation ability^{16,17,22,23} also played a relevant role in the initiating performance. This point is notably evidenced by comparing the final monomer conversions obtained with OXE-A and OXE-C. Thus, the FC of OXE-A is higher than that of OXE-B (62%) and OXE-C (57%). If one includes the number of photoactivated molecules, which is correlated with the absorption of the PI (the slopes are similar), one cannot conclude that the methyl radical has the best initiation properties. OXE-D is more reactive as OXE-A, OXE-B have a much lower absorbance but is still very reactive. This indicates that, in addition to fragmentation, absorption, steric aspects and stabilization of the fragments^{27,28} also play an important role. Note that the theory of stabilization of fragments²⁷ attributes poor radical transfer capabilities to all radicals where the radical is in an orbital orthogonal to an aromatic ring system.

Compounds	A ^{p1}	B ^{p1}	C ^{p1}	D ^{p1}	E	F ^{p2/p3}	G ^{p2}
λ_{\max} (nm)	371	370	370	370	371	371	371
ϵ_{\max} (10^4 L/(mol·cm))	1.65	1.20	1.55	1.50	1.70	1.40	1.30
FC (%)	64	62	59	64	62	48	50
Compounds	H ^{p2}	I	J ^{p3}	K ^{p3}	L ^{p4}	M ^{p4}	N
λ_{\max} (nm)	372	372	372	372	373	372	376
ϵ_{\max} (10^4 L/(mol·cm))	2.00	1.40	1.20	1.40	1.30	1.10	2.20
FC (%)	54	46	40	49	53	48	26

Note: Structurally similar compounds are identified by p1, p2, p3, and p4. p1 for aliphatic esters; p2 for simple aryls; p3 for aryls with mesomeric groups, and p4 extended aromatic systems.

TABLE 1 Absorption characteristics of OXE A-M in acetonitrile (10^{-4} mol/L) and final double bond content in photopolymerization reactions.

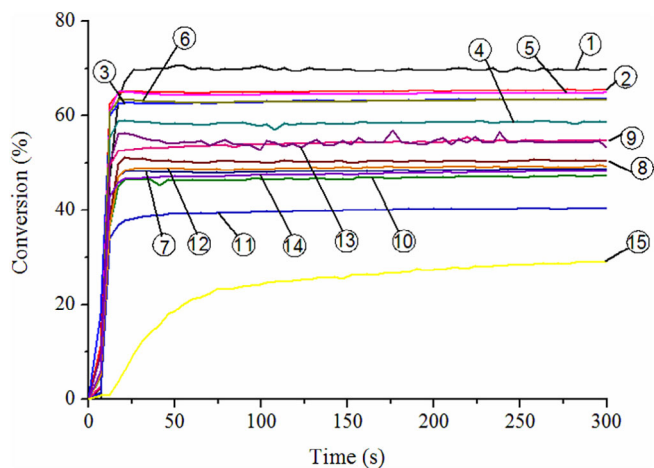


FIGURE 2 Photopolymerization profiles of TMPTA (acrylate functions conversion vs. time) obtained in laminate ($\approx 25 \mu\text{m}$) in the presence of OXEs-based PIs ($1 \times 10^{-5} \text{ mol/g}$) and TPO ($1 \times 10^{-5} \text{ mol/g}$) under LED@405 nm irradiation: ① TPO, ② OXE-A, ③ OXE-B, ④ OXE-C, ⑤ OXE-D, ⑥ OXE-E, ⑦ OXE-F, ⑧ OXE-G, ⑨ OXE-H, ⑩ OXE-I, ⑪ OXE-J, ⑫ OXE-K, ⑬ OXE-L, ⑭ OXE-M, ⑮ OXE-N.

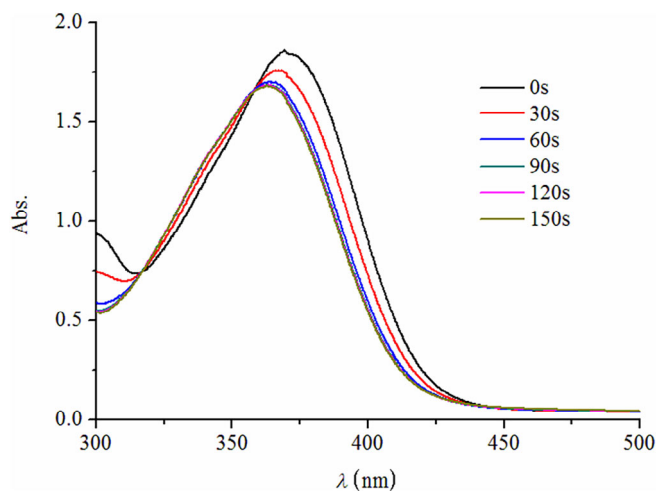


FIGURE 3 Steady-state photolysis of OXE-A upon irradiation at 405 nm in acetonitrile ($1 \times 10^{-4} \text{ mol/L}$).

In order to evaluate the photochemical properties of these OXEs, steady-state photolysis measurements were carried out at room temperature (see Figures 3 and S1–S5). As shown in Figure 3, the maximal absorbance of OXE-A decreased upon irradiation at 405 nm during the first 30 s. Meanwhile, new compounds were generated during the photolysis process, as revealed by the hypsochromic shift detected for the maximum absorption wavelength. When exposed to the LED@405 nm, RCOO[•] radicals are generated by homolytic cleavage of OXEs, which can be detected by ESR (electron spin resonance,

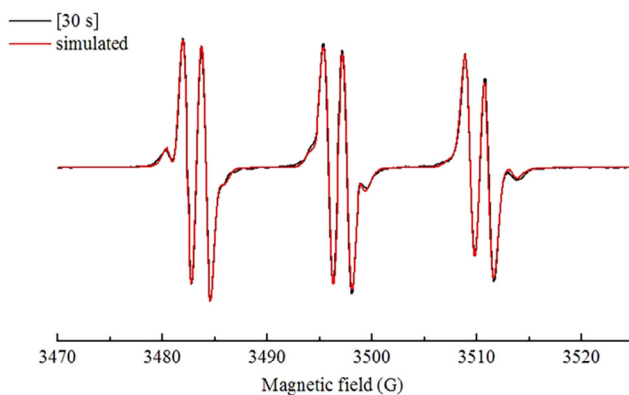


FIGURE 4 ESR spectrum of OXE-A under irradiation of LED@405 nm (after 30 s) in *tert*-butylbenzene ($1 \times 10^{-3} \text{ mol/L}$) and PBN (phenyl-*N-tert*-butyl nitrene).

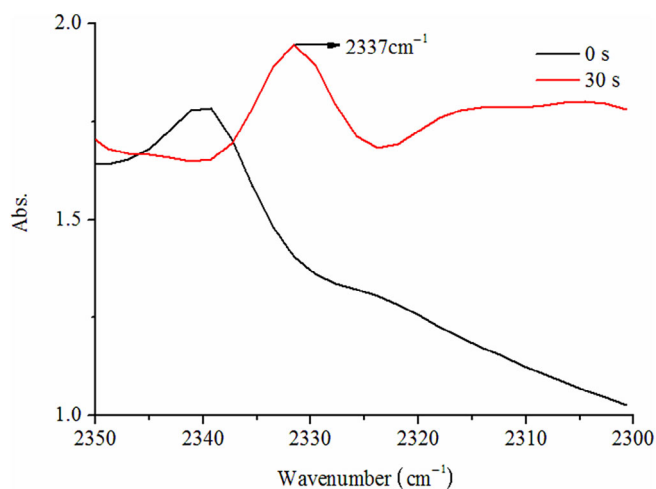
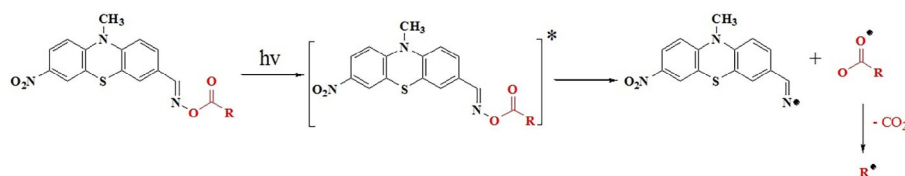


FIGURE 5 FTIR spectra of TMPTA in the presence of OXE-A ($1 \times 10^{-5} \text{ mol/g}$) before (black) and after (red) 30 s irradiation of LED@405 nm.

See Figure 4). After 30-s irradiation, the hyperfine coupling constants of the main radical adduct (81.0%) were $\alpha_{\text{N}} = 13.5 \text{ G}$ and $\alpha_{\text{H}} = 1.8 \text{ G}$ which were identified as being an acetoxy radical ($\text{CH}_3\text{COO}^{\bullet}$). These hyperfine coupling constants are in full agreement with the literature data.^{22,29} These active species can quickly undergo a decarboxylation reaction by releasing CO_2 and create active R[•] radicals, which can induce a polymerization process.

The release of CO_2 could be detected by FTIR (see Figure 5). Notably, OXE-A exhibited different infrared spectra during the photopolymerization processes at $t = 0 \text{ s}$ and $t = 30 \text{ s}$. The absorption peak at 2337 cm^{-1} was attributed to the generation of CO_2 .³⁰ Moreover, no peak was observed for TPO and OXE-N upon light irradiation. This proves the generation of CO_2 by nitrophenothiazine-based OXEs when exposed to LED@405 nm. According to these results above,



SCHEME 3 Proposed mechanism for the photocleavage of nitrophenothiazine-based OXEs.

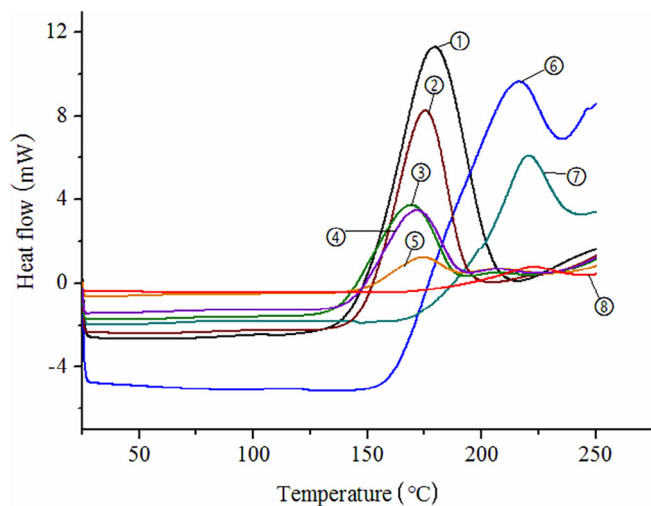


FIGURE 6 DSC curves of OXEs and TPO in TMPTA (1×10^{-5} mol/g): ① OXE-A, ② OXE-E, ③ OXE-F, ④ OXE-M, ⑤ OXE-I, ⑥ OXE-N, ⑦ TPO, ⑧ pure TMPTA (without any initiator). There is almost no difference in the onset temperature of the sample containing TMPTA and no initiator, clearly indicating that TPO is not a thermal initiator. A DSC experiment for commercial OXE02 can be found in Figure S6.

the photoinitiation mechanism of nitrophenothiazine-based OXEs upon light irradiation was proposed and is shown in Scheme 3.^{22,31,32}

Upon light exposure, OXEs can be promoted to the excited state, resulting in the dissociation of the N—O bond of OXEs (cleavage reaction) generating acyloxy and imino radicals. Furthermore, acyl radicals can undergo a decarboxylation reaction, and highly reactive radicals (R^\bullet) can be generated, promoting the polymerization of acrylate monomers.

3.4 | Thermal initiation abilities of OXEs

As reported in previous works, several OXEs-based PIs were found to exhibit dual photo/thermal initiator behaviors.³² Therefore, this point was examined with the different OXEs reported in this work, and the new proposed OXEs were evaluated for their thermal initiation abilities. Specifically, the thermal initiation abilities of these OXEs in TMPTA were measured by DSC under dark conditions (see Figure 6).

Compared to pure TMPTA (without OXE or any initiator; Figure 6, curve 8), it is found that the polymerization can be initiated at lower temperature in presence of OXEs, for example, for OXE-A, the polymerization can be initiated at $\sim 130^\circ\text{C}$ with a maximal temperature $\sim 180^\circ\text{C}$. The commercially available oxime-esters OXE01 and OXE02 show similar behavior. This thermal initiating ability of OXE is better than for TPO or the acrylate itself (curve 7) or the oxime (OXE-N) (curve 6). It can be assumed that with TPO, fragmentation occurs “only” from the photoactivated state or a vibrational band that cannot be achieved by thermal activation. Thus, OXEs can also be used as a thermal initiator. Details concerning the heating experiments can be found in the [Supporting Information](#). This dual initiating ability (light and heat) was useful for the curing of opaque samples with: (i) a primary fast photopolymerization in the irradiation areas and (ii) a secondary curing of the shadow areas by subsequent thermal treatment. An example will be given below. Due to the high onset of the oxime ester reactivity ($T > 130^\circ\text{C}$) the storage stability of the samples containing oxime esters is most likely not influenced by the initiator. For example, storage stability tests with Luperox P (tertbutylperoxybenzoate) at 50°C for more than 10 days did not lead to any significant conversion of the double bonds, although the reaction temperature of this initiator is much lower with an onset below 120°C .

3.5 | Preparation of carbon fiber composite and glass fiber composite

Since most of the carbon fibers are black, the light penetration is thus limited. Therefore, carbon fiber composite materials were usually prepared by thermal curing. In this work, based on its outstanding dual initiation behavior (see above), OXE-A (1×10^{-5} mol/g) was used to prepare carbon fiber composites using TMPTA as the monomer with the following ratio: TMPTA/carbon fiber (50 wt%/50 wt%). Due to the limited light penetration inside this black formula, photopolymerization only occurred on the top surface (first step). Thus, the specimen (dimension $100 \times 10 \times 2$ mm) was irradiated with a LED@405 nm up and down for 10 min individually. Then, in the second step, the sample was cured in an oven at 150°C for 15 min. With the dual-functional

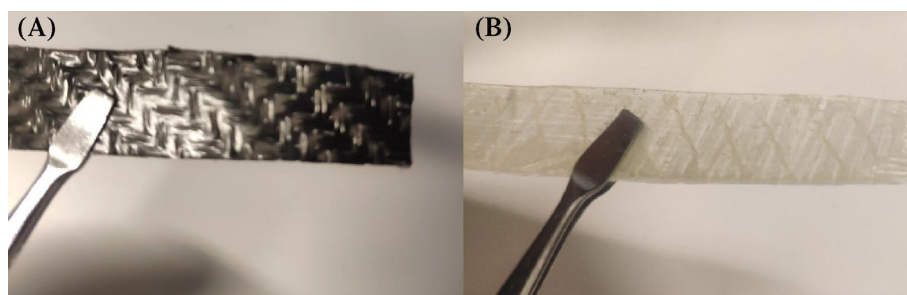


FIGURE 7 Pictures of (A) carbon fiber composite and (B) glass fiber composite produced using OXE-A (1×10^{-5} mol/g) as a dual photo and thermal initiator. The rigidity of the material has been increased, but due to the high functionality of the model resin chosen, the production of samples for mechanical analysis is difficult (visible cracks may appear in the organic matrix).

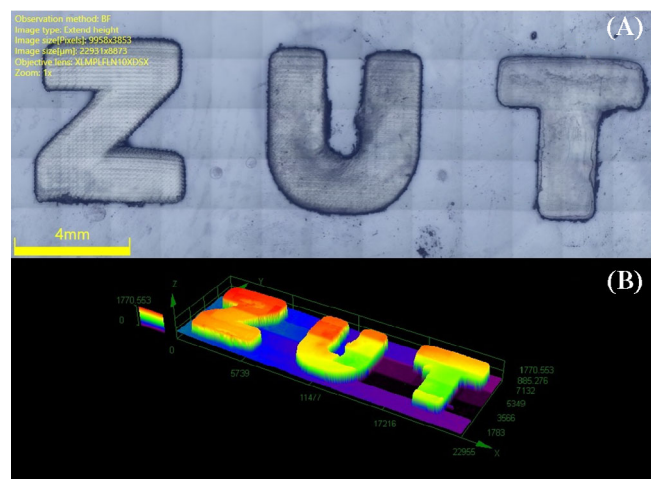


FIGURE 8 Characterization of the letter pattern “ZUT” by numerical optical microscopy: (A) top surface morphology and (B) 3D overall appearance of the color pattern.

initiator, carbon fiber composites were successfully formed as the final product (See Figure 7A). Due to the fact that glass fibers are partly transparent, the glass fiber TMPTA system could be prepared directly by photopolymerization. The same formulation can also be used for the preparation of glass fiber composites upon irradiation with a LED@405 nm for 15 min (see Figure 7B), that is, only one step is required (the photochemical one).

3.6 | Direct laser write of the OXE/TMPTA system

Finally, the letter patterns “ZUT” for Zhongyuan University of Technology were written by 2D direct laser write (see Figure 8). A laser diode with an intensity of 110 mW/cm^2 was used as the irradiation source. OXE-A (1×10^{-5} mol/g) was selected as the photoinitiator, and TMPTA was chosen as the monomer. Some edges of the

character were deformed since OXE-A can act as a dual-functional (photo and thermal) initiator where thermal polymerization was taken place at the edge of the laser spot but the spatial resolution remains reasonable. The thickness of the printed pattern letters was about $1770 \mu\text{m}$. Remarkably, 3D objects could be easily printed, showing a great prospect for the OXE-A to be used as PI in the future. The potential advantage arising from the thermal initiation potential is particularly interesting when considering that thermal post-curing is often performed in 3D manufacturing, the time of which can be greatly reduced by using such oxime esters as initiators.

4 | CONCLUSIONS

In this work, 13 nitrophenothiazine-based OXEs were designed and synthesized as type I photoinitiators for the free radical photopolymerization of TMPTA upon irradiation of LED@405 nm. Their photoinitiation efficiencies were evaluated by RT-FTIR. Specifically, OXE-A achieved the highest final function conversion, thus showing a good photoinitiation efficiency when exposed to LED@405 nm, and exhibiting excellent light absorption properties at this wavelength. Based on its remarkable reactivity, OXE-A could be incorporated in formulations used for direct laser write, enabling to produce 3D letters with a reasonable spatial resolution. Furthermore, the photoinitiating mechanism was revealed by UV-visible absorption spectroscopy, ESR-ST and FTIR. Specifically, the releasing of CO_2 during photopolymerization indicates a photocleavage followed by a decarboxylation process occurred upon excitation. Therefore, this work reveals the importance of the decarboxylation process in the photoinitiation ability of the different OXEs and provides an achievable strategy for the development of novel and high-performance photoinitiators. Alternatively, their thermal stability and thermal initiation abilities were confirmed by DSC. OXE-A displayed a good dual photo/thermal initiation

ability, broadening its potential applications in industries. Especially the thermal initiation ability is interesting for 3D printing application which often includes a post-processing by heat treatment. In particular, the thermal initiation capability is interesting for 3D printing applications that often involve post-processing through heat treatment.

ACKNOWLEDGMENTS

This research project was supported by China Scholarship Council (CSC No. 201902425004).

ORCID

Jacques Lalevée  <https://orcid.org/0000-0001-9297-0335>

REFERENCES

- [1] P. Xiao, J. Zhang, F. Dumur, M.-A. Tehfe, F. Morlet-Savary, B. Graff, D. Gigmes, J.-P. Fouassier, J. Lalevée, *Prog. Polym. Sci.* **2015**, *41*, 32.
- [2] A.-H. Bonardi, F. Morlet-Savary, T. M. Grant, F. Dumur, G. Noirbent, D. Gigmes, B. H. Lessard, J.-P. Fouassier, J. Lalevée, *Macromolecules* **2018**, *51*, 1314.
- [3] J. Lalevée, N. Blanchard, M. A. Tehfe, F. Morlet-Savary, J. P. Fouassier, *Macromolecules* **2010**, *43*, 10191.
- [4] M. J. Moran, M. Magrini, D. M. Walba, I. Aprahamian, *J. Am. Chem. Soc.* **2018**, *140*, 13623.
- [5] A. A. Mousawi, F. Dumur, P. Garra, J. Toufaily, T. Hamieh, B. Graff, D. Gigmes, J.-P. Fouassier, J. Lalevée, *Macromolecules* **2017**, *50*, 2747.
- [6] P. Xiao, M. Frigoli, F. Dumur, B. Graff, J. P. Fouassier, D. Gigmes, J. Lalevée, *Macromolecules* **2014**, *47*, 106.
- [7] A. Kocaarslan, C. Kütahya, D. Keil, Y. Yagci, B. Strehmel, *ChemPhotoChem* **2019**, *3*, 1127.
- [8] X. Zuo, F. Morlet-Savary, M. Schmitt, D. Le Nouën, N. Blanchard, J.-P. Goddard, J. Lalevée, *Polym. Chem.* **2018**, *9*, 3952.
- [9] J. Lalevée, S. Telitel, P. Xiao, M. Lepeltier, F. Dumur, F. Morlet-Savary, D. Gigmes, J. P. Fouassier, *Beilstein J. Org. Chem.* **2014**, *10*, 863.
- [10] J. Lalevée, J. P. Fouassier, *Polym. Chem.* **2011**, *2*, 1107.
- [11] Z. Li, X. Zou, G. Zhu, X. Lui, R. Liu, *Appl. Mater. Interfaces* **2018**, *9*, 16113.
- [12] X. Allonas, F. Morlet, J. Lalevée, J. P. Fouassier, *Photochem. Photobiol.* **2006**, *82*, 88.
- [13] A. Bagheri, J. Jianyong, *ACS Appl. Polym. Mater* **2019**, *1*, 593.
- [14] C. Dietlin, S. Schweizer, P. Xiao, J. Zhang, F. Morlet-Savary, B. Graff, J.-P. Fouassier, J. Lalevée, *Polym. Chem.* **2015**, *6*, 3895.
- [15] J. Heng, A. Xiaode, T. Kun, Z. Tianyi, Z. Yan, Y. Shouyun, *Angew. Chem. Int. Ed.* **2015**, *54*, 4055.
- [16] Z.-H. Lee, F. Hammoud, A. Hijazi, B. Graff, J. Lalevée, Y.-C. Chen, *Polym. Chem.* **2021**, *12*, 1286.
- [17] F. Hammoud, Z. H. Lee, B. Graff, A. Hijazi, J. Lalevée, Y. C. Chen, *J. Polym. Sci.* **2021**, *59*, 1711.
- [18] R. Mallavia, R. Sastre, F. Amat-Guerri, *J. Photochem. Photobiol. A.* **2001**, *138*, 193.
- [19] E. F. David, L. Andrea, P. M. Jan, A. Kelterer, G. Gescheidt, B. K. Christopher, *Macromolecules* **2017**, *50*, 1815.
- [20] M. Rahal, H. Mokbel, B. Graff, J. Toufaily, T. Hamieh, F. Dumur, J. Lalevée, *Catalyst* **2020**, *10*, 1202.
- [21] A.-H. Bonardi, F. Bonardi, G. Noirbent, F. Dumur, D. Gigmes, C. Dietlin, J. Lalevée, *J. Polym. Sci.* **2020**, *58*, 300.
- [22] F. Hammoud, A. Hijazi, M. Schmitt, F. Dumur, J. Lalevée, *Eur. Polym. J.* **2023**, *188*, 111901.
- [23] F. Hammoud, N. Giacoletto, M. Nechab, B. Graff, A. Hijazi, F. Dumur, J. Lalevée, *Mater. Eng.* **2022**, *307*, 2200082.
- [24] Y. Miyake, H. Takahashi, N. Akai, K. Shibuya, A. Kawai, *Chem. Lett.* **2014**, *43*, 1275.
- [25] A. Mahmood, S. D. Khan, U. A. Rana, *Arab. J. Chem.* **2019**, *12*, 1447.
- [26] H. M. Jiang, Y. L. Zhao, Q. Sun, X. H. Ouyang, J. H. Li, *Molecules* **2023**, *28*(4), 1775.
- [27] M. Schmitt, *Macromol. Chem. Phys.* **2012**, *213*, 1953.
- [28] M. Schmitt, *Nanoscale* **2015**, *7*, 9532.
- [29] G. A. Russell, J. P. Lokensgard, *J. Am. Chem. Soc.* **1967**, *19*, 5059.
- [30] J. Kumar, S. F. D'Souza, *Talanta* **2008**, *75*, 183.
- [31] Z. H. Lee, S. C. Yen, F. Hammoud, *Polymer* **2022**, *14*, 5261.
- [32] L. Shaohui, X. Pu, F. Dumur, J. Lalevée, *Macromol. Rapid Commun.* **2021**, *10*, 207.

SUPPORTING INFORMATION

Additional supporting information can be found online in the Supporting Information section at the end of this article.

How to cite this article: X. Zhang, X. Peng, D. Zhu, Y. Zhang, M. Le Dot, S. Ozen, M. Schmitt, F. Morlet-Savary, P. Xiao, F. Dumur, J. Lalevée, *J. Polym. Sci.* **2023**, *1*. <https://doi.org/10.1002/pol.20230327>